

# Theoretical Study of the Neutral Hydrolysis of Hydrogen Isocyanate in Aqueous Solution via Assisted-Concerted Mechanisms

S. Tolosa Arroyo,\* A. Hidalgo Garcia, and J. A. Sansón Martín

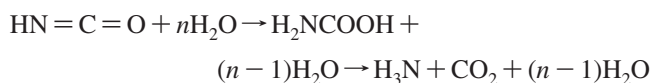
Departamento de Química. Universidad de Extremadura. 06071 Badajoz. Spain

Received: October 21, 2008; Revised Manuscript Received: December 21, 2008

A procedure is described for the theoretical study of chemical reactions in solution by means of molecular dynamics simulation, with solute–solvent interaction potentials derived from ab initio quantum calculations. We apply the procedure to the case of neutral hydrogen isocyanate hydrolysis,  $\text{HNCO} + 2 \text{H}_2\text{O} \rightarrow \text{H}_2\text{NCOOH} + \text{H}_2\text{O}$ , in aqueous solution, via the assisted-concerted mechanisms and the two-water model. We used the solvent as a reaction coordinate and the free-energy curves for the calculation of the properties related to the reaction mechanisms, with a particular focus on the reaction and activation energies. The results showed that the mechanism with two water molecules attacking the  $\text{C}=\text{N}$  bond is preferred to the mechanism with three waters forming a ring of eight members. In addition, the aqueous medium significantly reduces the activation barrier ( $\Delta G^\ddagger = 13.9$  kcal/mol) and makes the process more exothermic ( $\Delta G = -11.1$  kcal/mol) relative to the gas-phase reaction, increasing the rate constant of the process to  $k = 4.25 \times 10^5 \text{ s}^{-1}$ .

## 1. Introduction

The isocyanate hydrolysis reaction has been the subject of numerous experimental and theoretical studies<sup>1–21</sup> because of its interest for the polymer industry, the pharmaceutical industry, and agriculture.<sup>1</sup> It is also interesting because of its controversial reaction mechanism because it can react with water in different places depending on the number of water molecules involved in the structure of the transition state. The water molecule can attack the isocyanate at the  $\text{C}=\text{O}$  or the  $\text{N}=\text{C}$  group, the latter being the more favored when the reaction takes place with two or more water molecules. In this latter situation, initially carbamic acid  $\text{H}_2\text{NCOOH}$  is formed through a concerted mechanism (slow reaction step), followed by the rupture of the acid to give ammonia  $\text{NH}_3$  and carbon dioxide  $\text{CO}_2$  (fast reaction step):



When the reaction takes place with a single water molecule, the initial attack is on the  $\text{C}=\text{O}$  group to give an enolic intermediate  $\text{HN}=\text{C}(\text{OH})_2$  before forming carbamic acid in a second step:



Most studies of this hydrolysis reaction have been restricted to the gas phase, where the concerted mechanism assisted by a second water molecule leads to a six-member ring structure, which is favored over the eight-member ring formed by three water molecules, and is not as rigid as the four-member ring formed with a single water molecule.

An ab initio study of Lee et al.,<sup>19</sup> with STO-3G minimum bases and geometries derived from the semiempirical MINDO/3 method, showed that the activation barrier for the transition state with two water molecules is lower than that for the transition state with one water molecule, implying that the water dimer is

preferred over the water monomer in isocyanate hydrolysis. However, the activation barrier with three water molecules is similar to the two water molecule case, so that the reaction via the trimer may be competitive with the reaction via the dimer, although the formation of an eight-member ring makes the hydrolysis with two water molecules preferred entropically.

The first theoretical studies of isocyanate hydrolysis in aqueous solution were those of Raspoet et al.<sup>20,21</sup> using high-level ab initio methods and large basis sets. They concluded that the solvent effect as modeled by the Onsager SCRF approach,<sup>22</sup> and the polarized continuum method PCM<sup>23</sup> reduces the barrier energy less than expected, although a charge separation occurs in the transition state. Like Lee et al.,<sup>19</sup> Raspoet et al.<sup>20</sup> conclude that, whereas two water molecules in the form of a dimer seem to play the key role in the isocyanate hydrolysis, a third water molecule may be needed to facilitate the hydration. Specifically, there is a lowering of 10 kcal/mol in activation enthalpy relative to the reaction with two water molecules. This result is quite surprising because the transition state formed with three water molecules increases the entropy component of the barrier.

The latest theoretical studies of isocyanate hydrolysis are those of Ivanova and Muchall,<sup>24</sup> who use the “two water molecule” model in the gas phase and the hybrid density functional method (B3LYP) with the 6-31+G(2d,2p) basis set, confirming previous results that hydrolysis through a transition state with two water molecules takes place by the attack of the solvent on the  $\text{C}=\text{N}$  group. Although the barrier energy is reduced when the reaction passes through a transition state with three water molecules, one must not forget that the results presented were based only on the enthalpies of the systems. A study considering Gibbs free energies would increase the barrier by taking the entropy contribution into account, and the barrier may be higher when the transition state is formed with an eight-member ring.

Experimentally, a plot of the observed rate constant against the water concentration shows a second-order dependence on water.<sup>20</sup> The results confirmed that two molecules of water are involved in the rate-determining step over the entire concentra-

\* To whom correspondence should be addressed. Tel.: +34-924289401. Fax: +34-924275576. E-mail: santi@unex.es.

tion range. Water oligomers higher than the dimer seem to make no appreciable contribution to the reaction rate.

Given this context, the main objectives of the present study were: (a) to apply our methodological approach to this hydrolysis reaction to provide calculations of activation and reaction free energies in the absence of existing results for this process in solution; (b) to attempt to shed light on some debatable aspects of this reaction such as that the aqueous solvent only slightly modifies the energies of the process, and that the presence of a third water molecule forming part of the transition state reduces the activation barrier; and (c) to make some modifications to our methodology for the study of reactions in solution with several reactant and product molecules, in the present case to improve the treatment of the overlapping systems, and also to consider repulsive energy zones for the fit of interaction parameters.

## 2. Formalism and Calculation Details

Then we make a description of the methodology used in the calculation of the solute–solvent interaction potential and the free-energy curves, as was done in more detail earlier works.<sup>25–27</sup>

About a thousand values of the SCF and MP2 solute–water interaction energy  $U_{sw}$ , calculated with the 6-311++G\*\* basis set,<sup>28,29</sup> considering the BSSE effect<sup>30</sup> and a grid of points where the water molecule is placed in different positions,  $r_{ij}$ , respect to the solute, were used to obtain the  $A_{ij}$ ,  $B_{ij}$ , and  $q_i$  interaction parameters of the potential function:

$$U_{sw} = \sum_{ij} \frac{A_{ij}^{sw}}{r_{ij}^{12}} - \sum_{ij} \frac{B_{ij}^{sw}}{r_{ij}^6} + \sum_{ij} \frac{q_i^s q_j^w}{r_{ij}} \quad (1)$$

The net charges on each solute atom  $q_i^s$  were obtained using the ESIE procedure,<sup>31</sup> fitting the values of the Coulomb electrostatic component of the interaction energy  $U_{sw}(\text{ES})$  obtained from the variational scheme of Morokuma and co-workers<sup>32,33</sup>

$$U_{sw}(\text{ES}) = \sum_{ij} \frac{q_i^s q_j^w}{r_{ij}} \quad (2)$$

where the charges of the solvent water  $q_i^w$  are preassigned as the TIP3P charges.<sup>34</sup>

The Lennard–Jones parameters  $A_{ij}^{sw}$  and  $B_{ij}^{sw}$  are obtained in a similar way to  $q_i^s$ , but now the energies used in the fits are those that describe the exchange (EX) and polarization (PL) components of the interaction energy at the SCF level, and the dispersion (DIS) component related to the MP2 correlation energy:<sup>35</sup>

$$U_{sw}(\text{EX}) = \sum_{ij} \frac{A_{ij}^{sw}}{r_{ij}^{12}} \quad (3)$$

$$U_{sw}(\text{PL} + \text{DIS}) = - \sum_{ij} \frac{B_{ij}^{sw}}{r_{ij}^6} \quad (4)$$

To construct free-energy curves  $G_s$  from the simulations, we use as a reaction coordinate the difference in the solute–solvent interaction energy  $\Delta E_s$  of a given set of solvent molecules in the presence of the diabatic states of the reactant, transition state, and product,<sup>36</sup> for which one only needs the potential function  $U_{sw}$  that suitably describes this interaction. Thus, in the simulation of the solute in the A structure the interaction energy with all solvent molecules  $U_{sw,A}$  can be calculated for every

step of the simulation, and, at the same time, the energy  $U_{sw,B}$  is also obtained by replacing the B structure by the A structure.

$$\Delta E_s = U_{sw,A} - U_{sw,B} \quad (5)$$

When calculating the energy differences  $\Delta E_s$  between the two solute molecules (A and B) and the water solvent, and also in constructing the  $G_s$  free-energy curves, it must be taken into account that it is necessary during the simulation of one of the molecules to displace the other molecule to the position occupied by the first and to reorient it in order to reproduce the position of the atoms. In this respect, is suitable to use the transition-state geometry as a reference and then to displace the reactant (or product) at the geometric arrangement of the transition state but with their molecular geometries undeformed.

The difference  $\Delta E_s$  fluctuates during the MD simulation, and its values are collected as a histogram of the number of times  $N_s$  that a particular value  $\Delta e$  of the macroscopic variable  $\Delta E_s$  appears in the simulation. The probability  $P_s(\Delta e)$  of finding the system in a given configuration can be expressed in terms of the delta function  $\delta$  described in previous work:<sup>37,38</sup>

$$P_s(\Delta e) = \frac{\sum_{i=1}^{N_r} \delta(\Delta E_s(t_i) - \Delta e)}{N_s} \quad (6)$$

This allows us to compute the free energy  $G_s(\Delta e)$  and to build the free-energy curve for each case shown in figures of this work:

$$G_s(\Delta e) = -k_B T \ln P_s(\Delta e) \quad (7)$$

Next, a search is made for the polynomial function that best fits these free energies (considering the values  $\Delta e$  placed in the equilibrium zone and the region to higher energies), and the result is plotted. To obtain an analytical expression for the value of the activation energies, the reactant curve  $G_R$  is shifted at the point of minimum energy of the transition-state curve  $G_{TS}$  according to the work of Tachiya,<sup>39</sup> where the separation between the two minima is

$$\Delta G = G_{eq}^R - G_{eq}^{TS} = a(\Delta e_{eq}^{TS} - \Delta e_{eq}^R) + b(\Delta e_{eq}^{TS} - \Delta e_{eq}^R)^2 + c(\Delta e_{eq}^{TS} - \Delta e_{eq}^R)^3 + \dots \quad (8)$$

with  $\Delta e_{eq}^R$  and  $\Delta e_{eq}^{TS}$  being the most probable values of  $\Delta E$  in the free-energy curves  $G_R$  and  $G_{TS}$  respectively and  $a$ ,  $b$ , and  $c$  are the coefficients of the polynomial fit to the curve  $G_R$ . The procedure is similar for the activation energy of the inverse reaction except that now the curve that is shifted is  $G_p$ .

Finally, some simulation details merit commentary. Molecular dynamics simulations of an NVT ensemble of a solute molecule in an aqueous environment formed by about 205 water molecules were carried out at 298 K using the AMBER program.<sup>40</sup> The time considered for the simulations was 2000 ps with time steps of 0.1 fs. The first 1000 ps were taken to ensure that the equilibrium is reached completely, and the last 1000 ps were to store the configurations of the water molecules required for the determination of the thermodynamic properties studied in this work. The water molecules initially located at distances less than 1.6 Å from any solute atom were eliminated from the simulations. The long-range electrostatic interactions were treated by the Ewald method,<sup>41</sup> and the solutes were kept rigid using the shake algorithm.<sup>42</sup> A cutoff of 8 Å was applied to the water–water interactions to simplify the calculations, and periodic boundary conditions were used to describe the liquid state. The grid of points used to fit the interaction potential to

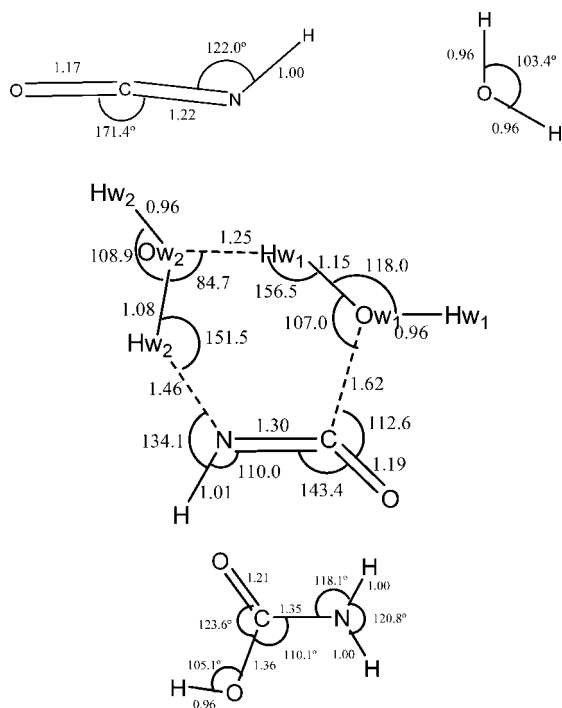


**Figure 1.** Reactant, transition state, and product structures.

the Lennard–Jones 12–6–1 function was obtained with SCF and MP2 energies using the *Gaussian/92* package,<sup>43</sup> and the decomposition of the interaction energies with the *Gamess* program.<sup>44</sup>

### 3. Results

**3.1. Structures and Interaction Parameters.** All geometries of the reactants, products, and transition states in the gas phase were optimized at MP2 level with the 6-311++G\*\* basis set starting from the standard geometries. An optimization of geometries in solution produces only small variations in angles and bond distances having an impact only on those quantum calculations realized on the solute molecules, but not so in the solute–solvent interaction energies used in this work to build free-energy curves. For the transition state, the geometry was confirmed by checking that there was one negative eigenvalue in the diagonalized Hessian, whereas for the reactants and products all of the frequencies were positive, resulting geometries in line with experimental values.<sup>45</sup>

The optimum geometry of the transition state formed with two water molecules is shown in Figure 1. It shows the reaction taking place with the simultaneous transfer of a hydrogen of one water molecule  $H_{W2}$  to the isocyanate nitrogen (electrophilic attack produced at 1.46 Å distance) and the oxygen of the other water molecule  $O_{W1}$  to the isocyanate carbon (nucleophilic attack produced at 1.62 Å distance). Both water molecules approach out of the HNCO molecular plane (the torsion angle  $H_{W2}\cdots N=C\cdots O_{W1}$  was found to be 19°), the  $N=C$  double bond is broken when the  $H_{W2}$  and  $O_{W1}$  atoms of the water molecules approach the N and C atoms of the isocyanate molecule respectively, and the oxygen of the  $C=O$  group bends in the direction opposite to the attacking water molecule and deforms the NCO angle to 143.4°. At the same time, a hydrogen bond ( $O_{W2}\cdots H_{W1}$ ) between the two water molecules is formed with a distance of 1.25 Å and an angle of 156.5°, resulting finally in a transition-state structure formed by a fairly flexible six-member ring.

**TABLE 1: Interaction parameters<sup>a,b</sup> of the Systems**

atoms	$A_{ij}$	$B_{ij}$	$q_i$
Isocyanate			
C	258 085.60	224.18	0.93
O	824 643.11	966.85	-0.48
N	1 397 806.90	1431.06	-1.02
H	1251.25	4.42	0.56
Carbamic Acid			
C	481 517.53	869.67	1.26
O(C)	642 260.12	799.24	-0.81
N	1 050 396.84	890.42	-1.43
H(N)	3852.14	28.67	0.61
O(H)	931 921.84	1028.06	-0.79
H(O)	32 722.03	112.83	0.53
Water			
O	581 931.56	594.83	-0.90
H	0.00	0.00	0.45
Transition State			
C	-177 435.72	527.73	1.18
O	1 313 550.13	659.90	-0.70
N	1 361 654.88	1278.59	-1.16
H	15 287.34	20.49	0.45
$O_{W1}$	1 191 506.90	1171.42	-1.02
$H_{W1}$	24 531.10	140.98	0.62
$H_{W1}^c$	39 565.02	24.60	0.68
$O_{W2}$	1 035 060.00	697.61	-1.14
$H_{W2}$	4772.97	81.36	0.59
$H_{W2}^c$	10 052.29	-245.06	0.56

<sup>a</sup> The van der Waals parameters (with the oxygen as the only interaction center) and charges in the solvent water are the TIP3P values of Jorgensen.<sup>34</sup> <sup>b</sup>  $A_{ij}$  in kcal Å<sup>12</sup> mol<sup>-1</sup> and  $B_{ij}$  in kcal Å<sup>6</sup> mol<sup>-1</sup>. <sup>c</sup> Hydrogen atoms in the ring.

Comparing these geometries with those of the reactant and product systems (Figure 1), one can say that in the case of isolated water the O–H bond in the ring and HOH angle increase from their initial values of 0.96 Å and 103.4°, respectively. The largest variations observed in the isocyanate geometry are the NCO angle, which loses its near linearity (passing from 171.4° to 143.4°), and the C–N distance, which increases from 1.22 Å in the reactant to 1.30 Å in the transition state. For the carbamic acid, the largest changes occur in the distance of the C–O simple bond, which increases from 1.36 Å in the product to 1.62 Å in the complex, and in the OCO angle which passes from 123.8° to 112.6° in the transition state. The other geometry parameters (the HNC and NCO angles and the N–C distance) also undergo significant changes with respect to the transition-state structure, although less marked.

Table 1 presents the interaction parameters, obtained with the 6-311++G\*\* basis set and optimum geometries in gas phase, used in the assisted-concerted mechanisms with the two-water model. There is a considerable variation in these parameters from one system to another, not only in atomic charges but also in the Lennard–Jones parameters. The greatest of these variations occur when we move from the transition state to the products. However, when the passage is from reactive to transition state the parameters on the atoms also change significantly, especially in the C and O atoms.

**3.2. Populations.** An analysis of the net charge for the isocyanate molecule in solution, obtained using the ESIE procedure,<sup>31</sup> shows the N atom to be the most negative and the C atom the most positive (Figure 2), which translates into a preference of the water reactant to attack at the  $C=N$  bond. Performing a population analysis on the transition state, one appreciates that the charge transfer occurs from the water hydrogen to the isocyanate nitrogen, and from the isocyanate

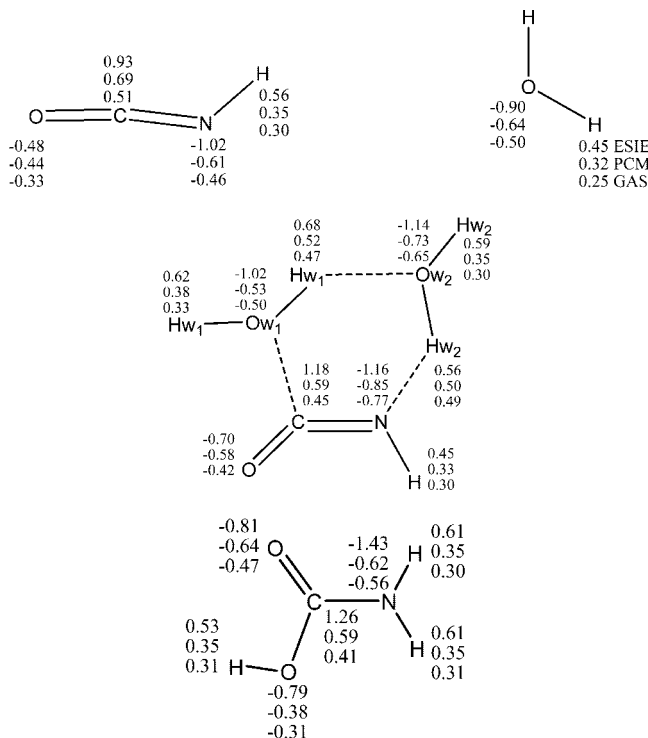


**Figure 2.** ESIE (top), PCM (middle), and gas-phase (bottom) charges.

**TABLE 2: Activation and Reaction Energies (kcal/mol) for the HNC(O)OH Hydrolysis**

method	ref	phase	$\Delta H^\ddagger$ ( $\Delta G^\ddagger$ )	$\Delta H_R$
MINDO/3	19	G	46.77	-16.30
STO-3G	19	G	22.92	
MP2/6-31G**	20	G	10.52	-18.18
MP2/6-311++G**	20	G	17.94	-12.67
QCISD(T)/6-31G**	20	G	12.44	-18.66
MP2/SCRF/6-31G**	20	S	14.35	-15.78
MP2/SCRF/6-311++G**	20	S	22.24	-10.76
MP2/PCM/6-31G**	20	S	15.07	-18.42
B3LYP/6-31+G(2d,3p)	24	G	12.9 (35.55)	

carbon to the water oxygen. Both the  $Hw_2 \rightarrow N$  and  $C \rightarrow Ow_1$  intermolecular charge transfers affect the populations of the other atoms in the water molecules, resulting in high charges on the  $Ow_2$  ( $\delta = -1.14$ ) and  $Hw_1$  ( $\delta = 0.68$ ) atoms that favored the formation of a hydrogen bond between the solvent molecules involved in the transition state.

The breaking of the  $Ow_1-Hw_1$  and  $Ow_2-Hw_2$  bonds in the molecular ring leads to a redistribution of the electronic charge so that the O and N atoms involved in the new bonds change their charges notably when the carbamic acid is finally formed.

In general, the ESIE atomic charges on the reactant, transition state, and product molecules are higher than those obtained in gas and solution phases with the Mulliken procedure, observing the effects previously mentioned for ESIE charges. This translates in a major solute-solvent interaction energies and solvation free energies when the ESIE charge is considered in the calculations.

**3.3. Energies.** An inspection of Table 2, which lists the previous results of other workers for this chemical reaction, shows that:

(a) The enthalpies depend on the method and basis used in the calculations. Thus, the semiempirical results are far from the ab initio calculations, and the minimal bases do not

**TABLE 3: Activation and Reaction Free Energies (kcal/mol) for the Isocyanate Hydrolysis<sup>a</sup>**

energies	reactant	transition state	product
PCM/ $\Delta G^\ddagger$	42.3 <sub>R-TS</sub>		61.8 <sub>TS-P</sub>
PCM/ $\Delta G_R$		-19.5	
MD/ $\Delta G^\ddagger$	13.9 (12.5) <sub>R-TS</sub>		25.0 (19.7) <sub>TS-P</sub>
MD/ $\Delta G_R$		-11.1 (-7.2)	

<sup>a</sup> Values refer to the isolated molecules (values in parentheses are for the reactants and products at the distance they have in the transition state but with interaction parameters of isolated systems).

adequately describe these energies. Likewise, the activation enthalpy seems more sensitive than the reaction enthalpy to the method and basis set used.

(b) The calculation of the reaction in solution modifies the results of the reaction and activation energies in the gas phase, although less than expected (about 2–4 kcal/mol). Considering the MP2 results with the basis 6-311++G\*\*, one can say that in these cases the aqueous medium increases the activation barrier making the process less exothermic, which is contrary to the real effect of the aqueous solvent in hydrolysis reactions.

(c) There is a significant lack of thermodynamics information for this process, especially for the energies in solution for which data are available only with continuum models. Only the work of Ivanova and Mutchall<sup>24</sup> studies the reaction free energy, although in the gas phase.

Table 3 lists the results for the activation and reaction free energies obtained with the PCM and MD procedure employed in this work. If one considers the PCM energies of these systems obtained from optimized energies in the gas phase, one observes a clearly exothermic reaction with a major activation barrier. However, because the reaction and activation values are higher than the theoretical and experimental energies available it will be useful to consider the solvent as discrete and take into account the entropy component, which is important for reactions in solution.

To solve this problem, we estimated the reaction ( $\Delta G_R$ ) and activation ( $\Delta G^\ddagger$ ) free energies using the average solute-solvent interaction energies per water molecule ( $\langle U_{sw} \rangle$ ) at each simulation step, following the procedure described in Section 2. These ( $\langle U_{sw} \rangle$ ) energies lead to values of the activation barriers and reaction energy in better agreement with those of previous studies (note that the results given in Table 2 refer to enthalpies) and significantly lower than those obtained by us in solution using the PCM model. Considering free energies, the reaction has to pass a barrier of 13.9 kcal/mol, although this step is compensated in energy by the 25.0 kcal/mol released to make the products, as shown in Table 3 and Figure 3 for the corresponding free-energy curves. One also observes from Table 3 that the results change by some kcal/mol depending on the distance between the reactant molecules for the direct reaction or the distance between product molecules for the inverse reaction.

The rate constant for isocyanate hydrolysis ranges from  $10^5$  to  $10^1$  s<sup>-1</sup> according to the system and the water concentration, which translates into an activation energy of 15 to 20 kcal/mol. Experimental results for phenyl isocyanate hydrolysis, obtained by Raspoet and Nguyen<sup>20</sup> for different concentrations of water at 25 °C, confirm that two molecules of water are involved in the rate-determining step, with the value of the rate constant being  $k = 2.48 \times 10^5$  s<sup>-1</sup> at  $[H_2O] = 35$  M. This study leads to activation barriers of around 14 kcal/mol, in good agreement with the activation barrier obtained by us in this present work.

Using the MP2/6-311++G\*\* free energies obtained in the gas phase for the different systems, we found values of  $\Delta G_R =$



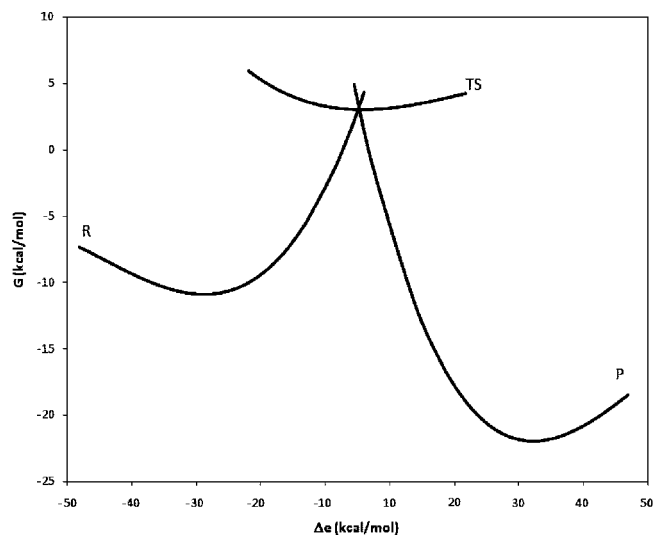


**Figure 3.** Free-energy curves for the reaction with two water molecules.

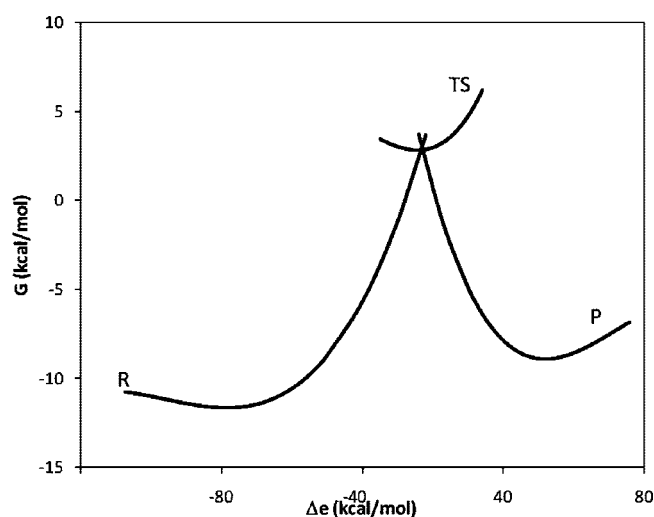


**Figure 4.** Free-energy curves for the reaction with three water molecules.

$-3.6$  kcal/mol and  $\Delta G^\ddagger = 36.2$  kcal/mol, which shows that the aqueous medium favors the reaction, decreasing the activation barrier and increasing the spontaneity of the process. Whereas this result contradicts those presented by other workers, it is in agreement with the idea that in general the aqueous medium favors the hydrolysis reaction.

To extend the good results obtained with our procedure for the isocyanate hydrolysis reaction to other mechanisms, in Figure 4 we show the activation and reaction free energies when considering a transition state comprising an eight-member ring with three water molecules, which has been optimized in the gas phase in this work. In this situation, although the activation barrier for the direct process increases by only 1 kcal/mol, in the reverse process it is reduced by nearly 14 kcal/mol, which makes the isocyanate hydrolysis reaction an endothermic process with a value of 3.1 kcal/mol. These results show the importance of using free energies instead of enthalpies because the entropy contributions from considering two or three water molecules as part of the transition state are quite different.

In sum, the free-energy curves of the species involved in the reaction provide a good description of the thermodynamics of

isocyanate hydrolysis in an aqueous medium. These curves, which are constructed on the basis of the solute–solvent interaction energies with the solvent fluctuation being chosen as a reaction coordinate, respond acceptably to the barrier and reaction energies of the process. Thus, to obtain favorable results for this reaction in solution one must take into account a transition state formed by two water molecules, and use free-energy curves where the solvent is treated as discrete and not as a continuum.

**Acknowledgment.** This research was sponsored by the Consejería de Infraestructuras y Desarrollo Tecnológico de la Junta de Extremadura (Project GRU08013).

## References and Notes

- (1) Ulrich, H. *The Chemistry and Technology of Isocyanates*; Wiley: New York, 1996.
- (2) Moodie, R. B.; Sansom, P. J. *J. Chem. Soc., Perkin Trans.* **1981**, 2, 664.
- (3) Oberth, A. E.; Brunner, R. S. *J. Phys. Chem.* **1968**, 72, 845.
- (4) Lillford, P. J.; Satchell, D. P. N. *J. Chem. Soc.* **1968**, 20, 889.
- (5) Lillford, P. J.; Satchell, D. P. N. *J. Chem. Soc.* **1968**, 20, 897.
- (6) Satchell, R. S.; Nyman, R. *J. Chem. Soc., Perkin Trans.* **1981**, 2, 901.
- (7) Poon, N. L.; Satchell, D. P. N. *J. Chem. Soc., Perkin Trans.* **1983**, 2, 1381.
- (8) Satchell, D. P. N. *J. Chem. Soc. Rev.* **1975**, 4, 231.
- (9) Lammiman, S. A.; Satchell, R. S. *J. Chem. Soc., Perkin Trans.* **1972**, 2, 2300.
- (10) Lammiman, S. A.; Satchell, D. P. N. *J. Chem. Soc., Perkin Trans.* **1974**, 2, 877.
- (11) Poon, N. L.; Satchell, D. P. N. *J. Chem. Res.* **1983**, 182, 1083.
- (12) Mader, P. M. *J. Org. Chem.* **1968**, 33, 2253.
- (13) Castro, E. A.; Moddie, R. B.; Sansom, P. J. *J. Chem. Soc., Perkin Trans.* **1985**, 2, 737.
- (14) Raspoet, G.; Nguyen, M. T. *J. Org. Chem.* **1998**, 63, 6867.
- (15) Schwetlick, K.; Noack, R.; Stebner, F. *J. Chem. Soc., Perkin Trans.* **1994**, 2, 599.
- (16) D'Silva, T. D. J.; Lopes, A.; Jones, R. L.; Singhawang, S.; Chan, J. K. *J. Org. Chem.* **1986**, 51, 3781.
- (17) Hegarty, A. F.; Ahern, E. P.; Frost, L. N.; Hegarty, C. N. *J. Chem. Soc., Perkin Trans.* **1990**, 2, 1935.
- (18) Williams, I. H.; Spanglas, D.; Femec, D. A.; Maggiora, G. M.; Schomn, R. L. *J. Am. Chem. Soc.* **1983**, 105, 31.
- (19) Lee, I.; Bon-Su, L.; Yae, Y. C. *J. Comput. Chem.* **1985**, 2, 79.
- (20) G.Raspoet, G.; Nguyen, M. T. *J. Org. Chem.* **1998**, 63, 6867.
- (21) G.Raspoet, G.; Nguyen, M. T. *J. Org. Chem.* **1998**, 63, 6878.
- (22) Wong, M. W.; Frisch, M. J.; Wiberg, K. B. *J. Am. Chem. Soc.* **1991**, 113, 4776.
- (23) Miertus, S.; Scrocco, E.; Tomasi, J. *Chem. Phys.* **1981**, 55, 117.
- (24) Ivanova, E. V.; Muchall, H. M. *J. Phys. Chem. A* **2007**, 111, 10824.
- (25) Tolosa, S.; Sansón, J. A.; Hidalgo, A. *J. Phys. Chem. A* **2007**, 111, 339.
- (26) Tolosa, S.; Corchado Martín-Romo, J. C.; Hidalgo, A.; Sansón, J. A. *J. Phys. Chem. A* **2007**, 111, 13515.
- (27) Tolosa, S.; Sansón, J. A.; Hidalgo, A. *Chem. Phys.* **2008**, 353, 73.
- (28) Ditchfield, R.; Hehre, W. J.; Pople, J. A. *J. Chem. Phys.* **1971**, 54, 724.
- (29) Hehre, W. J.; Ditchfield, R.; Pople, J. A. *J. Chem. Phys.* **1972**, 56, 2257.
- (30) Boys, S. F.; Bernardi, F. *Mol. Phys.* **1970**, 19, 553.
- (31) Tolosa, S.; Sansón, J. A.; Hidalgo, A. *Chem. Phys. Lett.* **2002**, 357, 279.
- (32) Kitaura, K.; Morokuma, K. *Int. J. Quantum Chem.* **1976**, 10, 325.
- (33) Umeyama, H.; Morokuma, K. *J. Am. Chem. Soc.* **1977**, 99, 1316.
- (34) Jorgensen, W. L.; Tirado-Rives, J. *J. Am. Chem. Soc.* **1988**, 110, 1657.
- (35) Moller, C.; Plesset, M. S. *Phys. Rev.* **1934**, 46, 618.
- (36) Carter, E. A.; Hynes, J. T. *J. Phys. Chem.* **1989**, 93, 2184.
- (37) King, G.; Warshel, A. *J. Chem. Phys.* **1990**, 93, 8682.
- (38) Kuharski, R. A.; Bader, J. S.; Chandler, D.; Sprik, M.; Klein, M. L.; Impey, R. W. *J. Chem. Phys.* **1988**, 89, 3248.
- (39) Tachiya, M. *J. Chem. Phys.* **1989**, 93, 7050.
- (40) Case, D. A.; Darden, T. A.; Cheatham, I. T. E.; Simmerling, C. L.; Wang, J.; Duke, R. E.; Luo, R.; Mert, K. M.; Wang, B.; Pearlman, D. A.; Crowley, M.; Brozell, S.; Tsui, V.; Gohlke, H.; Mongan, J.; Hornak, V.; Cui, G.; Beroza, P.; Schafmeister, C.; Caldwell, J.; Ross, W.; Kollman, P. A. *AMBER 8*; University of California: San Francisco, 2004.
- (41) Ewald, P. *Ann. Phys.* **1921**, 64, 253.

(42) Ryckaert, P.; Ciccotti, G.; Berendsen, J. J. C. *J. Comp. Phys.* **1977**, *23*, 237.

(43) Frisch, M. J.; Trucks, G. W.; Head-Gordon, M.; Gill, P. M. W.; Wong, M. W.; Johnson, B. G.; Schlegel, H. B.; Robb, M. A.; Replegle, E. S.; Gomperts, R.; Andres, J. L.; Raghavachari, K.; Binkley, J. S.; Gonzalez, C.; Martín, R. L.; Fox, D. J.; J., D. D.; Baker, J.; Stewart, J. J. P.; Pople, J. A., *GAUSSIAN-92 Revision D.3*; Gaussian Inc: Pittsburgh, PA, 1992.

(44) Dupuis, M.; Spangler, D.; Wendoloski, J. *GAMESS Program QG01*; *National Resource for Computations in Chemistry Software Catalog*; University of California: Berkeley, CA, 1980.

(45) Eyster, E. H.; Gillete, R. H.; Rockway, L. O. *J. Am. Chem. Soc.* **1940**, *62*, 3236.

JP809290J